

Coulomb blockade phenomena in electromigration break junctions

R. Sordan,^{a)} K. Balasubramanian, M. Burghard, and K. Kern

Max-Planck-Institut für Festkörperforschung, Heisenbergstr. 1, D-70569 Stuttgart, Germany

(Received 19 November 2004; accepted 25 May 2005; published online 29 June 2005)

Nanosized gap structures have been fabricated via electromigration-induced breaking of gold-palladium nanowires. The application of low breaking voltages resulted in gap junctions exhibiting single-electron tunneling signatures at low temperature (2 K), which are attributed to the formation of metallic nanoclusters during the electromigration process. Strikingly, the I - V characteristics of most samples displayed a close similarity to those typically attributed to electrical transport through single molecules contacted by incorporation into electromigration gaps. The finding that the breaking of bare nanowires alone is sufficient to create rich differential conductance features should be taken into account in future electrical studies on molecular-scale structures.

© 2005 American Institute of Physics. [DOI: 10.1063/1.1991988]

The continuous increase in the integration scale of semiconductor devices is a major driving force for the development of modern electronics. Present day commercial microprocessors consist of transistors with feature sizes as small as 90 nm, while in research laboratories transistor action has been demonstrated using a metal-oxide-semiconductor field effect transistor (MOSFET) with a gate length of just 6 nm.¹ The ultimate limit of integrated technology would be electronic devices comprising single molecules contacted between metal electrodes. Although it is currently not possible to fabricate such small junctions reliably on a large scale, various experimental approaches have been followed to gain a first insight into the electrical behavior of small molecular structures. Towards this end, scanning probe methods,²⁻⁴ sandwich junctions,^{5,6} as well as break-junctions created through mechanical^{7,8} or electromigration-induced⁹⁻¹² breaking of metallic nanowires have been employed to contact a small number of organic molecules and investigate their electrical properties.

Break junctions produced by electromigration are particularly useful owing to their compatibility with standard silicon technology and mechanical robustness. As an important advantage over mechanically controlled break junctions, nanogaps obtained via electromigration can be easily gated by an external electrode. In a typical electromigration experiment, the bias voltage across a thin metallic wire is ramped up to the point where it breaks due to the migration of metal atoms. For the purpose of contacting molecules, such wires are normally coated with self-assembled organic monolayers, with the aim of trapping molecules inside the junction during the subsequent breaking process.^{10,11} In these experiments, it is of great importance to distinguish the electrical current which flows through molecular states from tunneling currents across gap regions without molecules. Here, we demonstrate that even in the absence of intentionally introduced molecules, the break junctions reveal differential conductance features closely resembling those typically attributed to electrical transport through single molecules.

High resolution electron-beam lithography (EBL) was used to pattern 20-nm-wide metallic nanowires (MNWs). The wires were fabricated on a silicon (Si) substrate with a

100-nm-thick thermally grown SiO₂ layer on top. In order to avoid widening of the MNWs due to the proximity effect, electrodes required for electrical addressing of the nanowires were defined in a subsequent EBL step. The two EBL processes were aligned with the aid of a marker system patterned within the first step. The MNWs consisted of a 1-nm-thick titanium (Ti) adhesion layer and 7-nm-thick gold-palladium (60% Au+40% Pd) layer, implying a total conducting cross section of $\sim 8 \text{ nm} \times 20 \text{ nm}$.

The AuPd MNWs were broken by ramping the bias voltage until the electrical current density reached a critical (breaking) value J_B at which the wires fail. Identical results were obtained for all applied sweeping rates, which ranged between 1 and 6 mV/s. After the breaking point, the applied voltage was reset to zero, thus completing one breaking cycle. The current at the breaking point was found to be $I_B \sim 550 \mu\text{A}$ for the investigated MNWs, corresponding to a breaking current density of $J_B \sim 3.4 \times 10^{12} \text{ A/m}^2$. On the other hand, the effective applied breaking voltage $V_B = RI_B$ strongly depends on the total resistance $R = R_S + R_W$ of the circuitry connected to the voltage source, where R_S is the series resistance of the system and R_W is the resistance of the MNW. The resistance of the gap created within the MNW is much larger than R_S and R_W . Consequently, at the instance of breaking, the voltage V_B drops entirely across the gap region and influences the dynamics of the gap formation. Since the electric field in the gap is proportional to the applied voltage, shorter gaps are expected at lower breaking voltages. For this reason, the breaking properties of a large number of nanowires (~ 100) were studied using different breaking voltages. All breaking procedures and electrical measurements were performed at low temperature ($T = 2 \text{ K}$).

The breaking voltage can be expressed as $V_B = R_S I_B + \rho_W L_W J_B$, where ρ_W and L_W are the resistivity and length of the MNWs, respectively. The series resistance R_S and the length L_W were reduced by adjusting the geometry of the electrodes patterned in the second EBL step in order to lower the breaking voltage. The series resistance depends on the electrode width, thickness, and material, while the length of the MNWs is governed by the distance between the electrodes. The electrodes were made of Au and AuPd, with a thickness in the range of 8–70 nm, and a separation of $70 \text{ nm} < L_W < 10 \mu\text{m}$. For these dimensions, the measured

^{a)}Electronic mail: roman@fkf.mpg.de

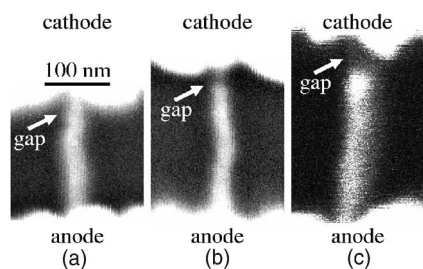


FIG. 1. SEM images of AuPd nanowires broken at (a) $V_B=1.0$ V, (b) $V_B=1.2$ V, and (c) $V_B=3.1$ V. The gaps are located in the vicinity of cathode. The scale bar applies to all three images.

breaking voltages were in the range $1 \text{ V} < V_B < 50 \text{ V}$.

The dependence of gap size on the breaking voltage was studied by scanning electron microscopy (SEM). In case of small breaking voltages ($V_B \sim 1$ V), the obtained gaps were too small to be resolved by SEM [Fig. 1(a)]. A very small low-bias resistance was found after the break [65 k Ω for the sample shown in Fig. 1(a)], suggesting a gap size in the sub-nanometer range. By comparison, slightly larger breaking voltages ($V_B \sim 1.2$ V) resulted in larger gaps (~ 10 nm), which could be resolved by SEM [Fig. 1(b)]. Inspection of the gap region reveals that it still contains metal, most likely in the form of very small clusters (a few nanometers in size).¹³ Under these breaking conditions, the electric field in the gap is apparently not sufficient to completely separate the metal clusters in proximity to the ends of the broken wire. The presence of the clusters explains why the low-bias resistance (~ 500 k Ω) is considerably smaller than the resistance estimated for direct tunnelling across the 10 nm wide gap (>1 G Ω). Indeed, the electrical properties of the break junctions resemble those of short gaps incorporating metallic islands which are introduced after the formation of the gaps.^{14–16} Finally, for breaking voltages larger than 2.5 V, the electric field in the gap creates a sufficiently strong electron wind to completely disrupt the wire. Hence, upon wire failure, the electrical current drops to a very low level. I - V curves measured after the break reveal featureless tunneling behavior with a typical low-bias resistance in the range above 1 G Ω . SEM images of such samples display relatively large gaps (~ 20 nm), with no detectable inclusion of metal clusters [Fig. 1(c)].

The small gaps obtained with $V_B < 2.5$ V were further investigated due to their relevance for contacting small molecules. These samples showed stable and reproducible electrical behavior. Figure 2(b) depicts a I - V curve of the sample whose breaking characteristic is shown in Fig. 2(a). The current fluctuations at voltages exceeding the breaking voltage used in the first cycle (1.2 V) are assigned to tiny reorganizations of the metal clusters inside the gap, caused by the electron flow. Upon ramping the bias voltage above ~ 1.4 V, an abrupt current decrease can be observed, which is attributed to structural rearrangements of the clusters, probably associated with the movement of clusters by the electron wind.¹⁷ As a consequence, the effective gap size is increased and the tunneling current significantly reduced. Moreover, we found that under opposite bias the clusters can be moved back to their original position, whereby the previous current level is restored, consistent with other reports.¹⁸ However, since the exact contact geometry is different, the features in the I - V curves are not exactly reproduced.

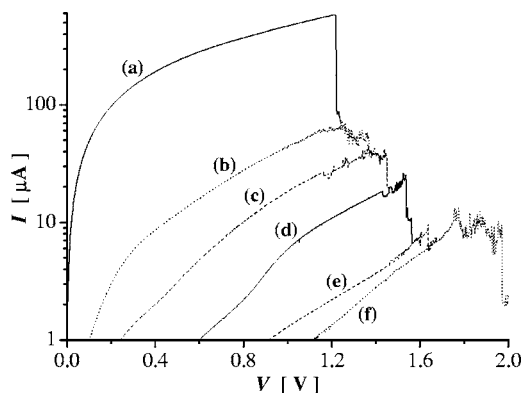


FIG. 2. Successive breaking characteristics of a AuPd nanowire at low temperature (2 K). Within each breaking cycle, the bias voltage is ramped up to the breaking point and reset back to zero after the break occurs. Initial I - V curve (a) is linear with a resistance of 2.1 k Ω . Second (b), third (c), fourth (d), fifth (e), and sixth (f) breaking curves pass through the breaking points of the previous cycle, confirming that the break geometry did not change between successive breaks.

The number of breaking cycles (six cycles in Fig. 2) required to fully separate all clusters inside the junction and hence maximally reduce the electrical current turned out to be dependent on the breaking voltage applied within the first cycle. Lower breaking voltages led to a smaller low-bias resistance after the first break, and a larger number of breaking steps were required afterwards. It is worth to note that similar step-like breaking characteristics as in Fig. 2 were observed even if the samples were broken in one run, i.e., without resetting the bias after each cycle.

After each breaking cycle, the electrical transport properties of the obtained structures were investigated in more detail. The differential conductance measured on the sample in Fig. 2 is plotted in Fig. 3. After the first and second breaks, multiple peaks are clearly visible [Figs. 3(b) and 3(c)]. The number and position of these peaks varied from sample to sample, reflecting different metal cluster configurations inside the ~ 10 nm gaps. After the third and fourth breaks [Figs. 3(d) and 3(e)], the metal clusters became further separated, leading to a decrease of the background tunneling, and the appearance of a prominent gap (0.2 V) in the g_d plot (corresponding to a low-bias resistance of 42 and 630 M Ω , respectively, for the present sample). These features were reproducibly found in many samples. After the fifth break,

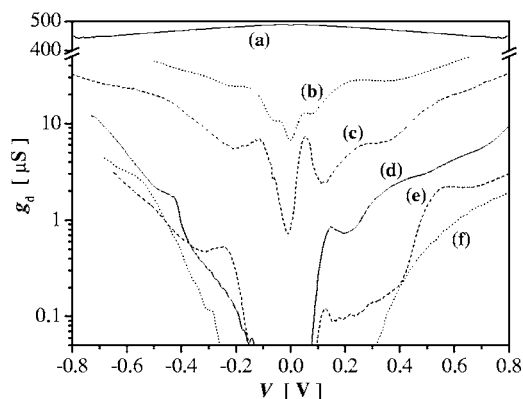


FIG. 3. Differential conductance g_d of the broken nanowire in Fig. 2, measured at low temperature (2 K), before breaking (a), and after the first (b), second (c), third (d), fourth (e), and fifth (f) break. Curves (a)–(f) match with the respective I - V curves (a)–(f) from Fig. 2.

the gap around zero bias has increased to ~ 0.6 V [Fig. 3(f)], which results in a very high low-bias resistance ($5\text{ G}\Omega$ for the present sample). This behavior suggests an almost complete separation of the clusters, giving rise to very low, featureless direct tunnelling current.

The discrete clusters located within the 10 nm gaps can be modeled as capacitors in a multiple tunnel junction formed between the electrodes.¹⁴ For such a configuration, Coulomb charging dominates the transport properties, as confirmed through the observation of Coulomb gap and differential conductance peaks in Figs. 3(d) and 3(e). From the measured Coulomb gap of ~ 0.2 V, the average size of the clusters is estimated¹⁴ to be ~ 3 nm, which is of the same order as the grain size of the evaporated thin AuPd film, and below the resolution limit of the SEM used in this study (5 nm). The irregular spacing between the Coulomb peaks is attributed to the presence of more than two tunnel junctions,^{14,19} and/or the influence of quantized electron states in small metal clusters.^{20–22}

In conclusion, the electromigration-induced breaking behavior of metallic nanowires was investigated at low temperature for different breaking voltages. At low breaking voltages, nanometer-sized metal clusters remain in the gap after the break, leading to Coulomb blockade phenomena at low temperatures. The observed differential conductance features bear a striking similarity to those frequently attributed to charge transport through single molecules between two metal electrodes. These results underline the importance to exercise caution when interpreting electrical transport data obtained from nanogaps fabricated in the presence of molecular layers.

The authors are grateful to T. Reindl for technical assistance. This work has been supported by the EU projects NANOTCAD (Contract No. IST-1999-10828) and QIPDDF-ROSES (Contract No. IST-2001-37150).

¹B. Doris, M. Jeong, T. Kanarsky, Y. Zhang, R. A. Roy, O. Dokumaci, Z. Ren, F.-F. Jamin, L. Shi, W. Natzle, H.-J. Huang, J. Mezzapelle, A. Mo-

- cuta, S. Womack, M. Gribelyuk, E. C. Jones, R. J. Miller, H.-S. P. Wong, and W. Haensch, *Tech. Dig. - Int. Electron Devices Meet.* **2002**, 267.
- ²D. Porath, Y. Levi, M. Tarabiah, and O. Millo, *Phys. Rev. B* **56**, 9829 (1997).
- ³X. D. Cui, A. Primak, X. Zarate, J. Tomfohr, O. F. Sankey, A. L. Moore, T. A. Moore, D. Gust, G. Harris, and S. M. Lindsay, *Science* **294**, 571 (2001).
- ⁴X. Xiao, B. Xu, and N. J. Tao, *Nano Lett.* **4**, 267 (2004).
- ⁵J.-O. Lee, G. Lientschnig, F. Wiertz, M. Struijk, R. A. J. Janssen, R. Egberink, D. N. Reinhoudt, P. Hadley, and C. Dekker, *Nano Lett.* **3**, 113 (2003).
- ⁶C. J.-F. Dupraz, U. Beierlein, and J. P. Kotthaus, *ChemPhysChem* **4**, 1247 (2003).
- ⁷M. A. Reed, C. Zhou, C. J. Muller, T. P. Burgin, and J. M. Tour, *Science* **278**, 252 (1997).
- ⁸J. Reichert, R. Ochs, D. Beckmann, H. B. Weber, M. Mayor, and H. v. Löhneysen, *Phys. Rev. Lett.* **88**, 176804 (2002).
- ⁹H. Park, A. K. L. Lim, A. P. Alivisatos, J. Park, and P. L. McEuen, *Appl. Phys. Lett.* **75**, 301 (1999).
- ¹⁰H. Park, J. Park, A. K. L. Lim, E. H. Anderson, A. P. Alivisatos, and P. L. McEuen, *Nature (London)* **407**, 57 (2000).
- ¹¹J. Park, A. N. Pasupathy, J. I. Goldsmith, C. Chang, Y. Yaish, J. R. Petta, M. Rinkoski, J. P. Sethna, H. D. Abruña, P. L. McEuen, and D. C. Ralph, *Nature (London)* **417**, 722 (2002).
- ¹²W. Liang, M. P. Shores, M. Bockrath, J. R. Long, and H. Park, *Nature (London)* **417**, 725 (2002).
- ¹³J. I. Gonzalez, T.-H. Lee, M. D. Barnes, Y. Antoku, and R. M. Dickson, *Phys. Rev. Lett.* **93**, 147402 (2004).
- ¹⁴W. Chen, H. Ahmed, and K. Nakazato, *Appl. Phys. Lett.* **66**, 3383 (1995).
- ¹⁵S. I. Khondaker and Z. Yao, *Appl. Phys. Lett.* **81**, 4613 (2002).
- ¹⁶K. I. Bolotin, F. Kuemmeth, A. N. Pasupathy, and D. C. Ralph, *Appl. Phys. Lett.* **84**, 3154 (2004).
- ¹⁷C. Durkan, M. A. Schneider, and M. E. Welland, *J. Appl. Phys.* **86**, 1280 (1999).
- ¹⁸S. J. van der Molen, M. L. Trouwborst, D. Dulic, and B. J. van Wees, CP685, *Molecular Nanostructures: XVII Int'l. Winterschool on Electronic Properties of Novel Materials*, edited by H. Kuzmany, J. Fink, M. Mehring and S. Roth, 2003, p. 511.
- ¹⁹E. Bar-Sadeh, Y. Goldstein, C. Zhang, H. Deng, B. Abeles, and O. Millo, *Phys. Rev. B* **50**, 8961 (1994).
- ²⁰M. E. Lin, R. P. Andres, and R. Reifenberger, *Phys. Rev. Lett.* **67**, 477 (1991).
- ²¹B. Wang, H. Wang, H. Li, C. Zeng, J. G. Hou, and X. Xiao, *Phys. Rev. B* **63**, 035403 (2000).
- ²²B. Wang, K. Wang, W. Lu, H. Wang, Z. Li, J. Yang, and J. G. Hou, *Appl. Phys. Lett.* **82**, 3767 (2003).